AIAA JOURNAL
Vol. 33, No. 1, January 1995

Flutter of an Infinitely Long Panel in a Duct

Ronald J. Epstein,* Ramakrishna Srinivasan,* and Earl H. Dowell†
Duke University, Durham, North Carolina 27706

The aeroelastic stability is examined of an infinitely long panel of finite width enclosed in a duct such that both the upper and lower surfaces of the panel are exposed to an inviscid, and compressible flow. The panel behavior is accounted for by small deflection plate theory, whereas the aerodynamic forces acting on the panel are described by the classical linearized small disturbance potential theory. As such, a self-consistent theoretical model is constructed for the asymptotic behavior of the panel. Two panel boundary conditions are considered; the panel is assumed to be either simply supported, or clamped along the side edges. For the simply supported case, rather extensive numerical results have been obtained. The effects of Mach number, air/panel mass ratio, and duct dimension on the flutter velocity are determined.

Nomenclature

a = speed of sound
a^* = a/c_0
b = panel width
c = wave speed
c_0 = reference wave speed, $2\pi(D/\rho_m h b^2)^{1/2}$
c^* = c/c_0
D = plate stiffness
E = modulus of elasticity
h = height of duct
h^* = nondimensional height of duct, h/b
h_p = panel thickness
L = panel length
l = wavelength
l^* = nondimensional wavelength, l/b
M = Mach number, U^*/a^*
m = number of modes
P = pressure
t = time
U = flow velocity
U^* = U/c_0
U^*_{cr} = critical flutter velocity
W = panel deflection
x = streamwise coordinate
y = spanwise coordinate
z = coordinate perpendicular to plane of panel
γ = separation constant
λ_b = nondimensional dynamic pressure, μU^{*2}
μ^* = $\rho b/\rho_m h$
ρ = fluid density
ρ_m = panel density
φ = velocity potential
ω = frequency
ω_0 = $(\pi/b)c_0$

Subscripts

R = real
I = imaginary
cr = critical

I. Introduction

THE aeroelastic stability is examined of an infinitely long panel of finite width enclosed in a duct such that both the upper and lower surfaces of the panel are exposed to an inviscid and compressible flow. The panel behavior is accounted for by small deflection plate theory, whereas the aerodynamic forces acting on the panel are described by the classical linearized small disturbance potential theory. Two panel boundary conditions are considered; the panel is assumed to be either simply supported or clamped along the side edges. For the simply supported case, rather extensive numerical results have been obtained for the flutter velocity indicating the effects of Mach number, air/panel mass ratio, and duct dimensions.

Mathematically, the present problem may be considered a generalization of the problem treated by Dowell[1] dealing with an infinitely long panel of finite width embedded in a baffle (rigid plane wall), with the upper surface exposed to an inviscid flow. In turn, the problem considered by Dowell is related to the work of Dugundji[2] et al. dealing with an infinitely long, infinitely wide panel resting on an elastic foundation. In the analyses discussed, as with the present problem, the critical wavelength corresponding to the first onset of instability is finite. The work by Miles[3] is also of interest, though for the geometry considered in Ref. 3, the flutter wavelength is found to be infinite. As will be shown, for the present problem, the critical wavelength is related to the panel width.

This type of panel structure can be considered an idealization of that found in an intake duct of a gas compression-expansion thrust device, such as a scram jet. In the physical case, however, the duct length is finite. The possible consequences of the infinite panel approximation are discussed later in the paper. Nevertheless, this analysis is relevant to the design of the next generation of aircraft engines, particularly the thrusters used on an hypersonic transport aircraft such as the National Aerospace Plane (NASP). Additionally, this analysis is not only relevant to aerospace applications, insofar as it can offer insight into many other types of internal duct flow problems; for example, such as those commonly found in nuclear power plants.

The experimental database for this type of panel flutter is rather limited. To summarize, a comprehensive experimental investigation of panel flutter was performed by Dowell and Voss[4] and another set of experiments exploring low supersonic Mach numbers was conducted by Muhlstein et al.[5] and Gaspers et al.[6] The experimental database from the experiments is limited to relatively small panel length to span ratios (L/b).

II. Problem Formulation

A. Simply Supported Case

The equation of motion of the panel is

$$D\left[\frac{\partial^4 W}{\partial x^4}+\frac{\partial^4 W}{\partial x^4 \partial y^4}+\frac{\partial^4 W}{\partial y^4}\right]+\rho_m h_p \frac{\partial^2 W}{\partial t^2}+p=0 \quad (1)$$

where the aerodynamic pressure on the panel p is determined from the well-known Bernoulli equation

$$p=-\rho\left[\frac{\partial \varphi}{\partial t}+U\frac{\partial \varphi}{\partial x}\right]_{Z=0} \quad (2)$$

Received Sept. 27, 1993; revision received March 23, 1994; accepted for publication April 17, 1994.

*Research Assistant, Department of Mechanical Engineering and Materials Science.
†J. A. Jones Professor and Dean, School of Engineering. Fellow AIAA.

and where the velocity potential φ satisfies the equation

$$\nabla^2\varphi - \frac{1}{a^2}\left[\frac{\partial^2\varphi}{\partial t^2} + 2U\frac{\partial^2\varphi}{\partial x\partial t} + U^2\frac{\partial^2\varphi}{\partial x^2}\right] = 0 \tag{3}$$

The boundary conditions on the panel deflection at the wide edges are

$$\begin{aligned} W(x,-b/2) &= 0 \\ W(x,b/2) &= 0 \\ \frac{\partial^2 W}{\partial y^2}\left(x,-\frac{b}{2}\right) &= 0 \\ \frac{\partial^2 W}{\partial y^2}\left(x,\frac{b}{2}\right) &= 0 \end{aligned} \tag{4}$$

and at each end of the panel, $W(\infty, y)$, $W(-\infty, y)$ are finite. The boundary conditions on φ are

$$\left.\frac{\partial\varphi}{\partial z}\right|_{z=0} = \frac{\partial W}{\partial t} + U\frac{\partial W}{\partial x} \qquad \text{for} \qquad |y| \le b/2 \tag{5}$$

$$\begin{aligned} \left.\frac{\partial\varphi}{\partial z}\right|_{z=h/2} &= 0 \\ \left.\frac{\partial\varphi}{\partial z}\right|_{z=-b/2,+b/2.} &= 0 \end{aligned} \tag{6}$$

and φ is bounded at $x \to +/-\infty$.

A panel deflection is assumed of the form

$$W = \hat{W}\cos\left(\frac{\pi y}{b}\right)e^{i(2\pi/l)(ct-x)} \tag{7}$$

The most general solution to the problem may be written as

$$W = \sum_n \hat{W}_n \cos\left(\frac{n\pi y}{b}\right)e^{i(2\pi/l)(ct-x)} + \sum_n \hat{W}_n \sin\left(\frac{n\pi y}{b}\right)e^{i(2\pi/l)(ct-x)} \tag{8}$$

Thus, strictly speaking, we are making a further approximation by limiting ourselves to the first term in the series; however, the error introduced is small and the retention of higher terms in the series seems hardly justified. Note that each term in the series Eq. (8) satisfies the plate boundary conditions.

Consistent with the assumed panel deflection shape is a velocity potential of the form

$$\varphi = \varphi(y,z)e^{i(2\pi/l)(ct-x)} \tag{9}$$

Equations (3), (5–7), and (9) constitute a well-defined mathematical boundary-value problem for φ which may be solved by standard methods as shown in the Appendix. Having determined φ, p may be determined through Eq. (2). Actually, for the present problem, our interest is not directly in p itself but rather in a weighted integral of p over the panel span; that is, Eq. (1) will be solved by the substitution of Eq. (7), multiplication by $\cos(\pi y/b)$, and integration over the panel width (i.e., a Galerkin solution in the spanwise variable). Thus, Eq. (1) becomes

$$\left\{D\left[\left(\frac{2\pi}{l}\right)^4 + 2\left(\frac{2\pi}{l}\right)^2\left(\frac{\pi}{b}\right)^2 + \left(\frac{\pi}{b}\right)^4\right] - \rho_m h_p\left(\frac{2\pi}{l}\right)^2 c^2\right\} \times \frac{b}{2}e^{i(2\pi/l)(ct-x)}\hat{W} = \int_{-\frac{b}{2}}^{\frac{b}{2}} -2p\cos\left(\frac{\pi y}{b}\right)\mathrm{d}y \tag{10}$$

In the Appendix it is shown that solving Eqs. (3), and (5–7) for φ using separation of variables and then by using Eq. (2) gives

$$\int_{-\frac{b}{2}}^{\frac{b}{2}} -2p\cos\left(\frac{\pi y}{b}\right)\mathrm{d}y = -\sum_{m=0}^{\infty}\frac{64\rho b^2}{\gamma}\left(\frac{U-c}{l}\right)^2 \times \frac{\hat{W}}{(4m-1)^2}\left[\frac{e^{-\gamma h^*}+1}{e^{-\gamma h^*}-1}\right]e^{i(2\pi/l)(ct-x)} \tag{11}$$

The factor of two appears in the left-hand integral term of Eq. (11) due to the pressure loading on both the upper and lower surfaces of the panel.

Canceling out common factors and employing a suitable nondimensionalization in Eq. (10), the characteristic equation is derived as the vanishing of the coefficient of $\hat{W}$:

$$\left(\frac{16}{l^{*4}} + \frac{8}{l^{*2}} + 1\right) - 16\left(\frac{c^*}{l^*}\right)^2 + (U^* - c^*)^2 F = 0 \tag{12}$$

where F and γ are defined as

$$F = \sum_{m=0}^{\infty} 128\mu^*\left[\frac{1}{(\gamma)(4m^2-1)^2(\pi l^*)^2}\right]\left[\frac{e^{-\gamma h^*}+1}{e^{-\gamma h^*}+1}\right]$$

and

$$\gamma = \pi\sqrt{m^2 - \left(\frac{1}{l^*}\right)^2\left[M^2\left(1-\frac{c^*}{U^*}\right)^2 - 1\right]}$$

Equation (12) may be expressed in functional form as

$$E(c^*, U^*, M, \mu^*, l^*) = 0 \tag{13}$$

In general, c^* may be a complex number, $c^* = c_R^* + ic_I^*$. For $c_I^* > 0$ the motion is stable; for $c_I^* = 0$ the motion is neutrally stable; and for $c_I^* < 0$ the motion is unstable. In general, it is found that for a given M, μ^*, h/b, and l/b the motion is neutrally stable for U^* sufficiently small but becomes unstable for some U^* sufficiently large. Of special interest is the value of l/b for given M, μ^*, and h/b which gives the smallest U^* for which unstable motion exists. This defines the critical or flutter condition and the corresponding values are designated U_{cr}^*, l_{cr}^*, and c_{cr}^*. The values of U_{cr}^* (flutter velocity), l_{cr}^* (flutter wavelength) and c_{cr}^* (flutter wave speed) have been calculated for a range of μ^* and M values.

B. Clamped Case

In this case, the governing equations remain the same [Eqs. (1–3), (5), and (6)], however, the boundary conditions on the panel deflection are modified [Eq. (4)] to account for the change in curvature at the panel boundary.[7] As such, the boundary conditions on the panel deflection at the wide edges are

$$\begin{aligned} W(x,-b/2) &= 0 \\ W(x,b/2) &= 0 \\ \frac{\partial W}{\partial y}\left(x,-\frac{b}{2}\right) &= 0 \\ \frac{\partial W}{\partial y}\left(x,\frac{b}{2}\right) &= 0 \end{aligned} \tag{14}$$

A panel deflection is assumed of the form

$$W = \hat{W}\left[1+\cos\left(\frac{2\pi y}{b}\right)\right]e^{i(2\pi/l)(ct-x)} \tag{15}$$

The most general solution to the problem, again, may be written as Eq. (8). Making a further approximation, we limit ourselves to the first two nonzero terms in the series; however, the error introduced is small and as with the simply supported case, the retention of higher order terms in the series seems hardly justified.

Consistent with the assumed panel deflection shape, the Eq. (9) velocity potential is chosen. Again, Eqs. (3), (5), (6), (9), and (15) constitute a well-defined mathematical boundary-value problem for φ which may be solved by standard methods (see Appendix for an example). Having determined φ, p may be determined through Eq. (2). Actually, for the present problem, as with the previous case, our interest is not directly in p itself but rather in a weighted integral of p over the panel span; that is, Eq. (1) will be solved by the substitution of Eq. (15), multiplication by $[1 + \cos(2\pi y/b)]$,

and integration over the panel width (i.e., a Galerkin solution in the spanwise variable). Thus, Eq. (1) becomes

$$\left\{D\left[\left(\frac{2\pi}{l}\right)^4+2\left(\frac{2\pi}{l}\right)^2\left(\frac{\pi}{b}\right)^2+\left(\frac{\pi}{b}\right)^4\right]-\rho_m h_p\left(\frac{2\pi}{l}\right)^2 c^2\right\}$$

$$\times\frac{b}{2}e^{i(2\pi/l)(ct-x)}\hat{W}=\int_{-\frac{b}{2}}^{\frac{b}{2}}-2p\left[1+\cos\left(\frac{2\pi y}{b}\right)\right]\mathrm{d}y \qquad (16)$$

Solving Eqs. (3), (5), (6), and (15), for φ using separation of variables and using Eq. (2) it can be shown that

$$\int_{-\frac{b}{2}}^{\frac{b}{2}}-2p\cos\left(\frac{\pi y}{b}\right)\mathrm{d}y=\left(-2\rho\hat{W}\left(\frac{2\pi}{l^2}\right)(U-c)^2 b\right)$$

$$\times\left[\frac{1}{\lambda_{20}}\frac{(e^{-2\lambda_{20}h^*}+1)}{(e^{-2\lambda_{20}h^*}-1)}+\frac{1}{2\lambda_{21}}\frac{(e^{-2\lambda_{20}h^*}+1)}{(e^{-2\lambda_{20}h^*}-1)}\right]e^{i(\frac{2\pi}{l})(ct-x)} \qquad (17)$$

Again, the factor of two appears in the right-hand integral term of Eq. (16) due to the pressure loading on both the upper and lower surfaces of the panel.

Canceling out common factors and employing a suitable nondimensionalization in Eq. (16), the following characteristic equation is derived as the vanishing of the coefficient of $\hat{W}$.

$$\left(\frac{1}{l^{*2}}+1\right)^2-\frac{c^{*2}}{l^{*2}}=\left(\frac{2\mu}{\pi}\frac{(U^*-c^*)^2}{l^{*2}}\right)$$

$$\times\left[\frac{1}{\lambda_{20}}\frac{(e^{-2\lambda_{20}h^*}-1)}{(e^{-2\lambda_{20}h^*}+1)}+\frac{1}{2\lambda_{21}}\frac{(e^{-2\lambda_{20}h^*}-1)}{(e^{-2\lambda_{20}h^*}+1)}\right] \qquad (18)$$

where

$$\lambda_{20}=\sqrt{-\left(\frac{1}{l^*}\right)^2\left[M^2\left(1-\frac{c^*}{U^*}\right)^2-1\right]}$$

$$\lambda_{21}=\sqrt{1-\left(\frac{1}{l^*}\right)^2\left[M^2\left(1-\frac{c^*}{U^*}\right)^2-1\right]} \qquad (19)$$

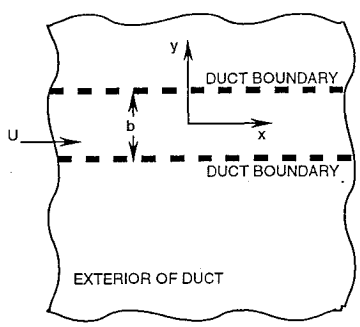

a) Top view

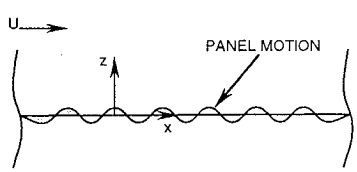

b) Side view

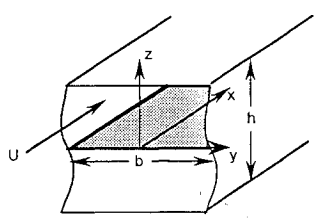

c) Cross-sectional view

Fig. 1 Panel geometry.

III. Numerical Results

Numerical results have only been obtained for the simply supported case. The clamped case has been left for future work; however, the methodology used for the simply supported case applies equally well to the clamped case.

A. Incompressible Case ($M = 0$)

For the incompressible case it is possible to find an analytical solution. One may solve Eq. (12) explicitly for

$$c^*=2U^*F\pm\left\{(2U^*F)^2-4\left(F-\frac{16}{l^*}\right)\right.$$

$$\left.\times\left(\frac{16}{(l^*)^4}+\frac{8}{(l^*)^2}+1+U^{*2}F\right)\right\}^{\frac{1}{2}} \qquad (20)$$

where F was previously defined in Eq. (12) and the following. Note that for $M = 0$, F is only a function of l^* and h^*, but not c^*; however, this is not the case for $M \neq 0$. The motion will become unstable, $c_I^* < 0$, when the quantity under the radical becomes negative, i.e., for

$$U^* > \left[\frac{4+(l^*)^2}{4(l^*)^2(-U^*F)^{\frac{1}{2}}}[16-U^*F(l^*)^2]^{\frac{1}{2}}\right] \qquad (21)$$

The F function was found to converge rapidly, and only the first few terms in the series were needed to provide sufficient accuracy. Note that $F < 0$.

In Fig. 2, U_{cr}^* is plotted as a function of mass ratio for a fixed duct dimension, $h^* = 1$. The corresponding values of l_{cr}^* and c_{cr}^* are shown in Figs. 3 and 4. The important points to note are the relative invariance of c_{cr}^* and the considerable variation that may occur in U_{cr}^* and c_{cr}^*. It is seen that the critical flutter wavelength is on the order of two times the panel width. Note also that $c_{cr}^* \to 0$ as $\mu \to 0$; i.e., the flutter wave speed goes to zero as the mass ratio approaches zero, and the instability becomes one of divergence. In other related studies,[1–3] this property has also been found.

Effect of Duct Dimension

It is interesting to examine the effect of duct dimension, namely, the ratio of duct height to width (h^*), on the preceding results which correspond to an h^* of unity. This is achieved by varying the value of h^* used in the F function. In Fig. 5, U_{cr}^* is plotted as a function of mass ratio for various values of h^*. The corresponding values of l_{cr}^* and c_{cr}^* are shown in Figs. 6 and 7. In the limit of large mass ratios, the values of U_{cr}^*, l_{cr}^*, and c_{cr}^* approach constant values independent of h^*. Both U_{cr}^* and l_{cr}^* are approximately two, whereas c_{cr}^* approaches unity. This limiting behavior seems to be consistent with the results for an isolated panel,[1] however, the limiting values for the present analysis are slightly higher than those found in the isolated panel case. This is due to the effect of the infinite rigid walls found at the panel boundaries which is not accounted for in the isolated panel analysis. Also, note that both U_{cr}^* and c_{cr}^* represent monotonically increasing and decreasing functions of h^*, respectively. Whereas the

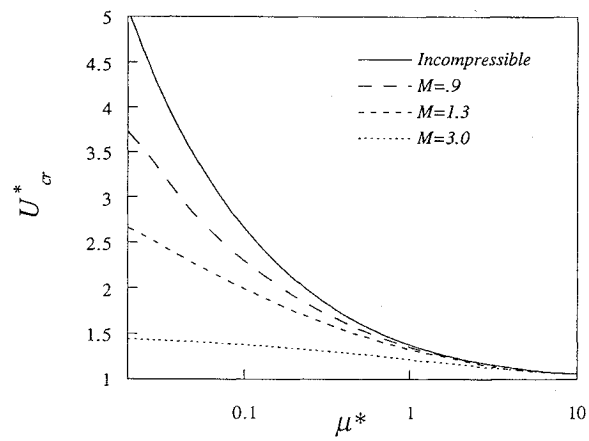

Fig. 2 Flutter velocity U_{cr}^* vs mass ratio μ^*.

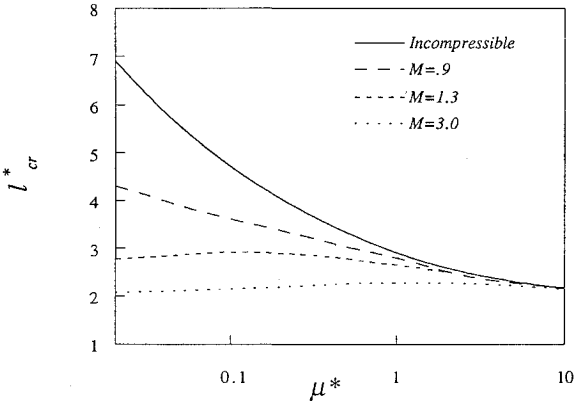

Fig. 3 Flutter wavelength l^*_{cr} vs mass ratio μ^*.

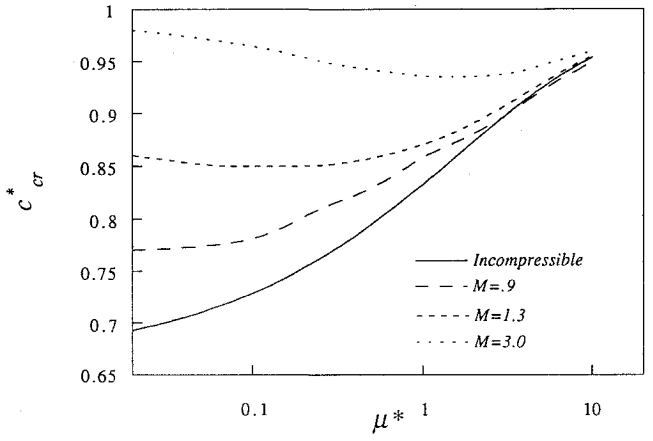

Fig. 4 Flutter wave speed c^*_{cr} vs mass ratio μ^*.

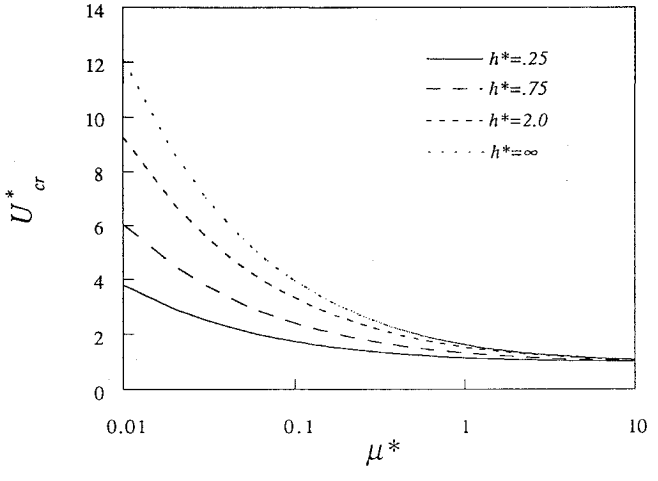

Fig. 5 Flutter velocity U^*_{cr} vs mass ratio μ^* for various duct heights $h^*, M = 0$.

dependence of l^*_{cr} on h^* is an increasing function until a duct height ratio on the order of two, then becomes a decreasing function. The limiting value of l^*_{cr} for large h^* is on the order of twice the panel width and is relatively invariant with respect to mass ratio, whereas U^*_{cr} and c^*_{cr} display considerable variation as functions of mass ratio. Again, this is similar to the isolated panel case. This behavior is shown in Figs. 8, 9, and 10, which show U^*_{cr}, l^*_{cr}, and c^*_{cr} plotted as functions of h^*. Clearly, l^*_{cr} is not a monotonic function of h^* until very large mass ratios.

In general, the duct height changes the load transmitted to the plate. As the duct height is decreased, the load transmitted to the plate is increased. This seems physically plausible because as the duct height decreases the energy in the system becomes more focused on the plate. In the limit as the duct height becomes very large the load on the plate is decreased, consistent with the results of Ref. 1.

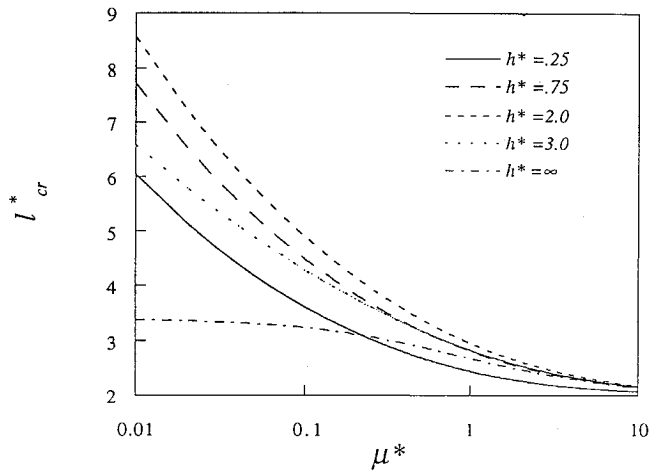

Fig. 6 Flutter wavelength l^*_{cr} vs mass ratio μ^* for various duct heights $h^*, M = 0$.

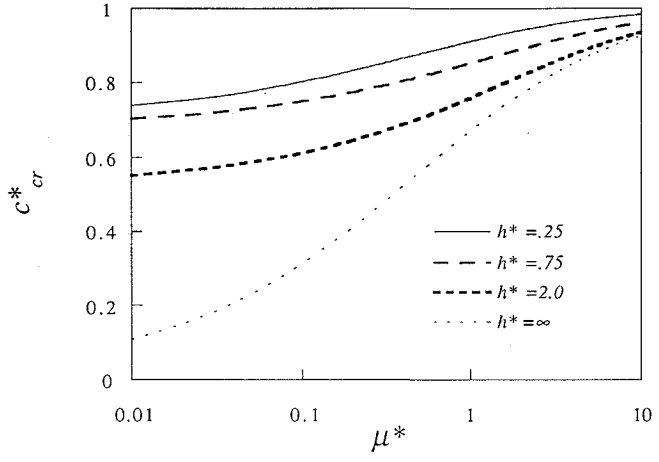

Fig. 7 Flutter wave speed c^*_{cr} vs mass ratio μ^* for various duct heights $h^*, M = 0$.

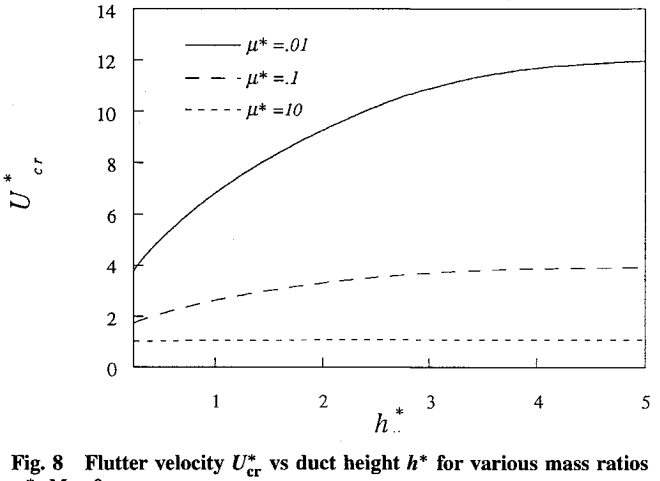

Fig. 8 Flutter velocity U^*_{cr} vs duct height h^* for various mass ratios $\mu^*, M = 0$.

B. Compressible Case ($M \neq 0$)

There are a several interesting mathematical and physical questions that arise with respect to the eigenvalue spectrum of the characteristic equation, Eq. (12), for the compressible case. Many of these are not of sufficiently general interest to warrant inclusion in the present paper. Here, the discussion is restricted to those results which describe the neutrally stable and unstable motions of the panel and to those which are pertinent to the determination of the practical flutter boundary.

For $M \neq 0$, F becomes a function of c^*, l^*, and M. Thus, for the examination of the boundary between neutrally stable and unstable

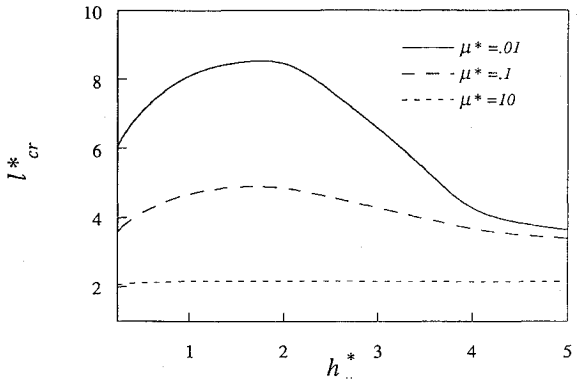

Fig. 9 Flutter wavelength l^*_{cr} vs duct height h^* for various mass ratios $\mu^*, M = 0$.

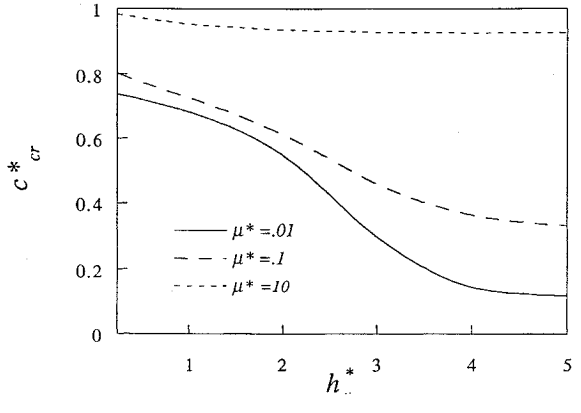

Fig. 10 Flutter wave speed c^*_{cr} vs duct height h^* for various mass ratios $\mu^*, M = 0$.

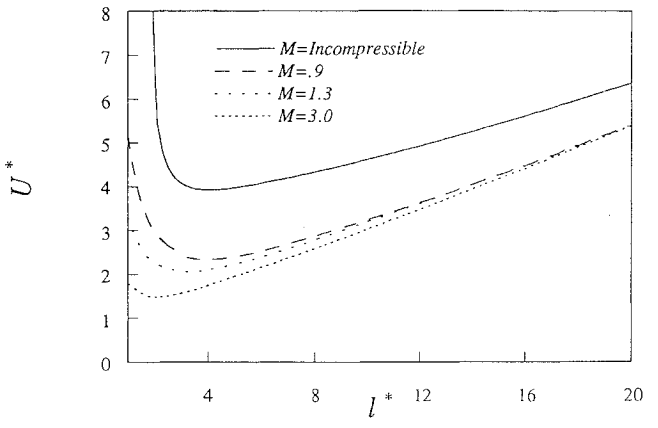

Fig. 11 Flow velocity U^* vs wavelength l^*, $\mu^* = 0.1$.

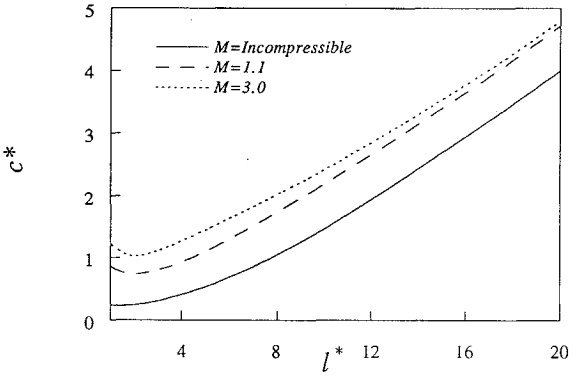

Fig. 12 Wave speed c^* vs wavelength l^*, $\mu^* = 0.1$.

motion for a panel, one may solve Eq. (12) readily by a graphical method. In doing so, it is convenient to introduce the following definitions:

$$S \equiv \left(\frac{16}{l^{*4}} + \frac{8}{l^{*2}} + 1\right) - 16\left(\frac{c^*}{l^*}\right)^2 \tag{22}$$

$$A \equiv (U^* - c^*)^2 F(\mu^*) \tag{23}$$

Thus, Eq. (12) may be rewritten simply as

$$A(c^*, U^*, M, \mu^*, l^*) \equiv S(c^*, l^*) \tag{24}$$

For fixed M, l^*, and μ^* (or U^*), A and S are plotted as functions of c^* for various U^* (or μ^*). The intersections (multiple) of A and S determine the eigenvalues (multiple) of c^*. However, for sufficiently large U^* (or μ^*) no intersection is possible for real c^*; and at c^* values corresponding to acoustic resonant duct modes, no intersection is possible for imaginary c^*. At the highest value of U^* (or μ^*), for which real values of c^* are solutions, the curves A and S are tangent; i.e.,

$$\frac{dA}{dc^*} = \frac{dS}{dc^*} \tag{25}$$

or, from Eq. (13),

$$\frac{dE}{dc^*} = 0 \tag{26}$$

At this point, two of the eigenvalues have coalesced. Thus, the boundary between stable and unstable motion is given by the two conditions

$$E = 0 \tag{27}$$

and

$$\frac{dE}{dc^*} = 0 \tag{28}$$

Now varying l^*, for fixed h^*, M, and μ^*: U^*_{cr}, l^*_{cr}, c^*_{cr} may now be determined. Shown in Fig. 11 is the relationship between U^* and l^* for various Mach numbers at a specified mass ratio. In all cases, $h^* = 1$. A smooth functional dependence of U^* on l^* is evident, additionally, there is a global minimum present for U^*. This minimum represents the U^* critical value (U^*_{cr}) for the specified Mach number and mass ratio. As such, the associated l^* value is the critical value (l^*_{cr}). By varying μ^* and M, the complete U^*_{cr} curve may be generated. Figure 12 shows the dependence of c^* on l^*. Again, the c^* curve is well behaved. The value of c^* corresponding to the l^*_{cr} value is the c^* critical value (c^*_{cr}). The results of such calculations are presented in Figs. 2–4 and Figs. 13–15 to show the effects of mass ratio and Mach number on the (nondimensional) flutter velocity, wavelength, and wave speed.

First consider U^*_{cr}. As shown in Fig. 2, U^*_{cr} decreases monotonically with increasing μ^*. Considering Fig. 13, for $\mu^* \to \infty$, $U^*_{cr} \to 1$ for all M. For $\mu^* \to 0$, $U^*_{cr} \to \infty$ for $M < 1$, and U^*_{cr} remains finite for $M > 1$, as discussed in Ref. 1. For $M \ll 1$, a better parameter than U^*_{cr} (for small μ^*) is a form of nondimensional dynamic pressure, namely, $\lambda_{b_{cr}}$, as discussed in Ref. 1. One may conclude that, for small μ^*, when $M \ll 1$, $\lambda_{b_{cr}}$ is approximately constant. Whereas for $M \gg 1$, U^*_{cr} is approximately constant. Also, for large μ^*, U^*_{cr} is essentially constant.

Now consider l^*_{cr}. In Fig. 3, it is plotted as a function of μ^* for several M. As may be seen, l^*_{cr} has a relatively small variation, in fact, $l^*_{cr} \to 2$ as $\mu^* \to \infty$ or $M \to \infty$. Indeed, the critical flutter wavelength is on the order of twice the panel width for all Mach numbers and mass ratios, as depicted in Fig. 14. As pointed out in Ref. 1, $l^* = 2$ may be identified as the wavelength corresponding to the minimum natural wave speed. Thus, the flutter wavelength is approximately equal to that corresponding to the minimum natural wave speed for all μ^* and M.

Now, consider the quantity c^*_{cr}, see Fig. 15. In Fig. 4, c^*_{cr} also is shown as a function of μ^* for several M. For $\mu^* \to \infty$, $c^*_{cr} \to 1$ for all M. For $\mu^* \to 0$, $c^*_{cr} \to 0$ for $M < 1$, whereas $c^*_{cr} \to 1$ for $M > 1$. In general, one may conclude that for $M \gg 1$, c^*_{cr} is relatively independent of μ^*; whereas for $M \ll 1$, it is relatively

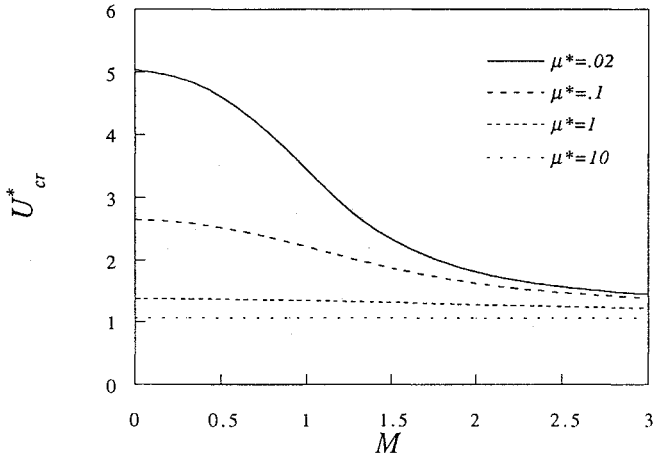

Fig. 13 Flutter velocity U^*_{cr} vs Mach number M.

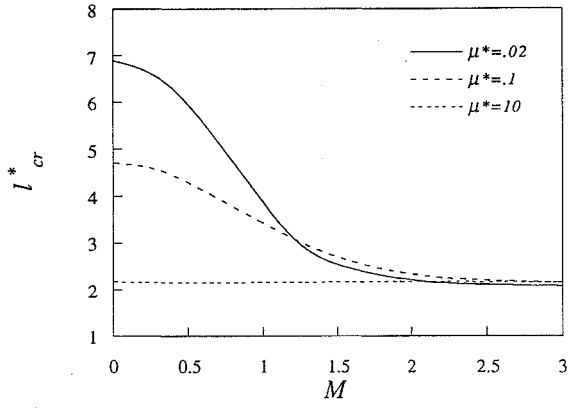

Fig. 14 Flutter wavelength l^*_{cr} vs Mach number M.

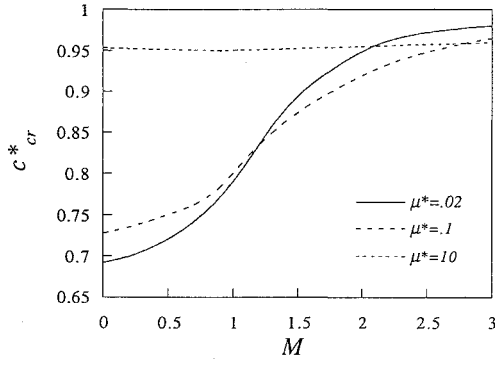

Fig. 15 Flutter wave speed c^*_{cr} vs Mach number M.

invariant with M and is increasing monotonically with μ^*, as shown in Fig. 15.

IV. Discussion of Analyses

Aside from the intrinsic interest which the present problem possesses, it is of considerable interest as a possible asymptotic solution to the problem of a long, narrow panel of finite length in a duct-type enclosure. Strictly speaking, it should be pointed out, what has been done here is to construct a self-consistent solution for a long narrow panel in a duct using the technique described in Ref. 1. That is to say, it has been shown that the critical modes have wavelengths that are of the order of twice the panel width, and the effect of duct height has been concluded to be merely a change in load intensity transmitted to the plate. Thus, it would seem physically plausible that the effect of end supports on a panel whose length is large compared to its width should be negligible on these modes. This was found to be true for a similar problem in Ref. 2. However, there is no a priori certainty that this will be true. The question is raised as to whether an infinitely long panel analysis is adequate to describe the behavior of a long but finite length panel. Additional analytical work and experimental work is clearly needed, both to assess the infinitely long panel model, as well as to consider alternative means to attack the low aspect ratio plate problem. As discussed in Ref. 7, for sufficiently high Mach number there are local (structural boundary layer) leading- and trailing-edge effects that may erode the accuracy of an infinitely long panel model.

V. Conclusions

The present work has described the flutter analysis of an infinitely long plate of finite width in a duct with the upper and lower surfaces exposed to an inviscid, potential flow. The major results are as follows.

1) A self-consistent theoretical model has been constructed for the asymptotic behavior of a long, narrow panel of finite width in a duct.

2) Numerical results have been obtained for flutter velocity (or dynamic pressure) indicating the effects of Mach number and mass ratio as well as duct dimension.

3) Additional work, both analytical and experimental, is needed to determine the relationship between the results for an infinitely long panel and a long but finite panel.

Appendix: Solution of the Aerodynamic Problem

Through Eqs. (3), (5), (6), (8), and (9), one can deduce the following boundary value problem for $\hat{\varphi}$:

$$\hat{\varphi}_{zz} + \hat{\varphi}_{yy} + (2\pi/l)^2[(U - c/a)^2 - 1]\hat{\varphi} = 0 \qquad \text{(A1)}$$

where

$$\hat{\varphi}_z\big|_{z=0} = -i(2\pi/l)(U-c)\cos(\pi y/b)\hat{W} \qquad |y| < (b/2)$$
$$\hat{\varphi}_z\big|_{z=\frac{h}{2}} = 0 \qquad \text{(A2)}$$
$$\hat{\varphi}_y\big|_{y=\pm\frac{b}{2}} = 0$$

Using separation of variables, assume $\hat{\varphi}(y, z) = F(y)G(z)$; then Eq. (A1) becomes

$$(F_{yy}/F) + (G_{zz}/G) + (2\pi/l)^2[(U - c/a)^2 - 1] = 0 \qquad \text{(A3)}$$

Let

$$F_{yy}/F = -\lambda_1^2 \qquad \text{(A4)}$$

where λ_1 is a constant of integration. From the third component of Eq. (A2), it is seen that

$$\left.\frac{\partial F}{\partial y}\right|_{y=\pm\frac{b}{2}} = 0 \qquad \text{(A5)}$$

The solution of Eq. (A4) is $F = A\cos(\lambda_1 y) + B\sin(\lambda_1 y)$. Applying boundary condition (A5) we see that $B \equiv 0$ and $A \neq 0$, if and only if

$$\lambda_{1n} = 2n\pi/b \qquad \text{(A6)}$$

for any n. Using only the even in y cosine terms for $F(\equiv \hat{W}$, matching panel surface), it follows that

$$F_n = \cos(2\pi n y/b) \qquad \text{(A7)}$$

Now from Eqs. (A3) and (A6),

$$G_{zz}/G = \lambda_{2n}^2 \qquad \text{(A8)}$$

where

$$\lambda_{2n}^2 = \lambda_{1n}^2 - \left(\frac{2\pi}{l}\right)^2\left[\left(\frac{U-c}{a}\right)^2 - 1\right] \qquad \text{(A9)}$$

It follows from the second boundary condition of Eq. (A2) that

$$\left.\frac{\partial G}{\partial z}\right|_{z=\frac{h}{2}} = 0 \tag{A10}$$

and, therefore, solving Eq. (A8) and applying boundary condition (A10), we find that

$$G(z) = C(e^{-\lambda_{2n}z} + e^{\lambda_{2n}(z-h)}) \tag{A11}$$

where C is yet to be determined.

Now from the first of the boundary conditions of Eq. (A2), and using Eqs. (A6) and (A11), we have

$$\begin{aligned}\left.\hat{\varphi}_z\right|_{z=0} &= \sum_n F_n(y)\left.\frac{\partial G_n}{\partial z}\right|_{z=0} \\ &= \sum_n C_n\left(-\lambda_{2n} + \lambda_{2n}e^{-\lambda_{2n}h}\right)F_n(y) \\ &= -i\left(\frac{2\pi}{l}\right)(U-c)\cos\left(\frac{\pi y}{b}\right)\hat{W}\end{aligned} \tag{A12}$$

where we recognize that for every F_n, there is a corresponding λ_{1n} and λ_{2n} and for every λ_{2n} there is a corresponding G_n. It follows that $\hat{\varphi} = \sum_n F_n G_n$. Now multiply both sides of Eq. (A12) by $\cos[(2m\pi y)/b]$ and integrate between $-b/2$ and $b/2$ to determine C_n.

$$\begin{aligned}&\sum_{n=0}^{\infty}\int_{-\frac{b}{2}}^{\frac{b}{2}} C_n\lambda_{2n}[e^{-\lambda_{2n}h} - 1]\cos\left(\frac{2n\pi y}{b}\right)\cos\left(\frac{2m\pi y}{b}\right)\mathrm{d}y \\ &= -i\hat{W}\left(\frac{2\pi}{l}\right)(U-c)\int_{-\frac{b}{2}}^{\frac{b}{2}}\cos\left(\frac{\pi y}{b}\right)\cos\left(\frac{2m\pi y}{b}\right)\mathrm{d}y\end{aligned} \tag{A13}$$

Using the orthogonality of $\cos[(2m\pi y)/b]$, C_n is readily found from Eq. (A13). After integration and algebraic manipulation, $\hat{\varphi}$ is determined to be

$$\begin{aligned}\hat{\varphi} = \sum_{m=0}^{\infty}\hat{W}\left(\frac{i(-1)^m 8}{\lambda_{2m}[4m^2-1]}\right)\frac{\left(\frac{(U-c)}{l}\right)}{(e^{-\lambda_{2m}h}-1)} \\ \times (e^{\lambda_{2m}(z-h)} + e^{-\lambda_{2m}z})\cos\left(\frac{2m\pi y}{b}\right)\end{aligned} \tag{A14}$$

Utilizing Bernoulli's equation, Eq. (2), and recalling Eq. (9), one may finally compute

$$\begin{aligned}P(x,y,t) = \sum_{m=0}^{\infty}\hat{W}\left(\frac{16\pi\rho}{\lambda_{2m}}\right)\left(\frac{(U-c)}{l}\right)^2\left(\frac{(-1)^m}{[4m^2-1]}\right) \\ \times\frac{(e^{-\lambda_{2m}h}+1)}{(e^{-\lambda_{2m}h}-1)}\cos\left(\frac{2m\pi y}{b}\right)e^{i(2\pi/l)(ct-x)}\end{aligned} \tag{A15}$$

References

[1]Dowell, E. H., "Flutter of Infinitely Long Plates and Shells. Part I: Plates," *AIAA Journal*, Vol. 4, No. 8, 1966, pp. 1370–1377.

[2]Dugundji, J., Dowell, E. H., and Perkin, B., "Subsonic Flutter of Panels on a Continuous Elastic Foundation," *AIAA Journal*, Vol. 1, 1963, pp. 1146–1154.

[3]Miles, J. W., "On the Aerodynamic Stability of Thin Panels," *Journal of the Aeronautical Sciences*, No. 23, 1956, pp. 771–780.

[4]Dowell, E. H., and Voss, H. M., "Experimental and Theoretical Panel Flutter Studies in the Mach Number Range 1.0 to 5.0," U.S. Air Force TDR-63-449, 1963; also, *AIAA Journal*, Vol. 1, 1963.

[5]Muhlstein, L., Jr, Gaspers, P. A., Jr., and Riddle, D. W., "An Experimental Study of the Influence of the Turbulent Boundary Layer on Panel Flutter," NASA TN D-4486, 1968.

[6]Gaspers, P. A., Jr., Muhlstein, L., Jr., and Petroff, D. N., "Further Experimental Results on the Influence of the Turbulent Boundary Layer on Panel Flutter," NASA TN D- 5798, 1970.

[7]Dowell, E. H., *Aeroelasticity of Plates and Shells*, Kluwer, Dordrecht, The Netherlands, 1975.